Journal of Physics: Conference Series **625** (2015) 012004 doi:10.1088/1742-6596/625/1/012004

Using the coupled wake boundary layer model to evaluate the effect of turbulence intensity on wind farm performance

Richard J.A.M. Stevens[1,2], Dennice Gayme[1], Charles Meneveau[1]

[1]Department of Mechanical Engineering, The Johns Hopkins University, 3400 North Charles Street, Baltimore MD 21218, USA

[2] Department of Science and Technology and J.M. Burgers Center for Fluid Dynamics, University of Twente, P.O Box 217, 7500 AE Enschede, The Netherlands

E-mail: r.j.a.m.stevens@jhu.edu

Abstract. We use the recently introduced coupled wake boundary layer (CWBL) model to predict the effect of turbulence intensity on the performance of a wind farm. The CWBL model combines a standard wake model with a "top-down" approach to get improved predictions for the power output compared to a stand-alone wake model. Here we compare the CWBL model results for different turbulence intensities with the Horns Rev field measurements by Hansen *et al.*, Wind Energy 15, 183196 (2012). We show that the main trends as function of the turbulence intensity are captured very well by the model and discuss differences between the field measurements and model results based on comparisons with LES results from Wu and Porté-Agel, Renewable Energy 75, 945-955 (2015).

1. Introduction

For the design of wind farms it is important to understand the effect of the relative turbine positioning on the overall power output [1]. Two analytical approaches have been used for such evaluations. The first approach, is the use of classical wake models [2–8] to estimate the wind farm performance. Such models have been used in several wind farm optimization studies [9–12]. Wake models predict the wake deficits in the entrance region of the wind farm well, but have difficulty predicting the performance further downstream where many wakes interact [13–15]. "Top-down" models [16–18] can capture the vertical structure of the atmospheric boundary layer and the associated wake-atmosphere interactions in this fully developed regime of the wind farm better than wake models. Therefore "top-down" models have been used for the evaluation of the optimal spacing in very large wind farms [19, 20]. However, "top-down" models do not consider the effect of the relative turbine positioning [21, 22] on the wind farm performance. Previous works have used a one-way coupling between wake and "top-down" models [6, 17, 23] to improve the performance.

In this paper we use the recently introduced coupled wake boundary layer (CWBL) model [15, 22] to predict the influence of the turbulence intensity on the performance of Horns Rev. In particular, to investigate how well computationally inexpensive analytical models can predict the influence of this flow feature. The CWBL model combines the Calaf *et al.* [18, 24] "top-down" model and a classical wake model [3, 4, 6] through two-way coupling. The effect of the

relative turbine positioning is captured by the wake model part and the interaction between the wind farm and the atmospheric boundary layer by the "top-down" part. It has been shown that the CWBL model [15, 22] gives improved predictions over either of its constitutive parts for the turbine power production in the fully developed regime of the wind farm. In this proceeding we start with a very short review of the basic concepts of the CWBL model in section 2. In section 3 the CWBL model results for different turbulence intensities are compared with field measurement data for Horns Rev [25] and corresponding LES results by Wu and Porté-Agel [26]. Section 4 concludes the paper.

2. The generalized CWBL model

In the CWBL model both the wake (section 2.1) and the "top-down" (section 2.2) model have one parameter that needs to be determined. An iterative procedure (section 2.3) is used to calculate these parameters from the complementary part of the CWBL model to make sure that a consistent CWBL system is obtained. For a detailed description of the (generalized) CWBL model we refer the reader to Refs. [15, 22].

2.1. Wake model part

The classic wake model [2–4, 6, 7] assumes that wind turbine wakes grow linearly with downstream distance and uses the following expression for the velocity (which is simplified as a top-hat distribution) in the turbine wakes [2, 3, 5]:

$$u = u_0 \left(1 - \frac{1-\sqrt{1-C_\mathrm{T}}}{(1+k_\mathrm{w}x/R)^2}\right) = u_0 \left(1 - \frac{2a}{(1+k_\mathrm{w}x/R)^2}\right). \tag{1}$$

Here u_0 is the incoming free stream velocity, k_w is the wake expansion coefficient, R is the rotor radius, $C_\mathrm{T} = 4a(1-a)$ is the thrust coefficient with flow induction factor a, and x is the downstream distance with respect to the turbine, which is modeled as an actuator disk. Wake interactions are accounted for by adding the squared velocity deficits of interacting wakes [4]. The predicted normalized turbine power P_T/P_1 is given by

$$\frac{P_\mathrm{T}}{P_1} = \left(\frac{1}{N_\mathrm{d}} \sum_{k=1}^{N_\mathrm{d}} \frac{u(\mathbf{x}_{T,k})}{u_0}\right)^3. \tag{2}$$

Here the summation k is over all points (N_d) on the turbine disk and the velocity ratio is obtained by calculating the effect of all wind turbine wakes, including the wake interaction effects, at these locations. We use a uniform inflow, which is common in wake models. Computing the sum over the entire disk, instead of just considering the value at hubheight, ensures that the ground effect modeled by the image turbines sets in incrementally, i.e. there are no discontinuous changes in the wake behavior with increasing the streamwise distance.

The wake decay parameter at the entrance of the wind farm $k_{\mathrm{w},0}$ can be modeled as the ratio of friction velocity to the mean velocity at hubheight, which gives

$$k_{\mathrm{w},0} = \frac{\kappa}{\ln(z_\mathrm{h}/z_{0,\mathrm{lo}})}, \tag{3}$$

where $z_{0,\mathrm{lo}}$ is the roughness length of the ground surface, z_h the turbine hubheight, and $\kappa = 0.4$ is the von Kármán constant [2, 17, 27]. To match the wake expansion coefficient to the turbulence intensity, expressed based on the streamwise velocity fluctuations, we use the following logarithmic laws for the mean

$$\langle \overline{u} \rangle / u_* = \kappa^{-1} \ln(z/z_{0,\mathrm{lo}}) \tag{4}$$

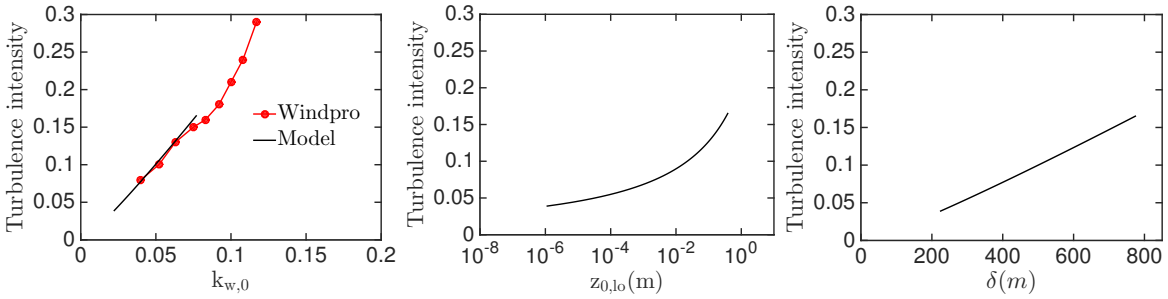

Figure 1. (a) The turbulence intensity at hubheight as a function of the wake expansion coefficient at the entrance of the wind-farm, $k_{w,0}$. The data points give the recommended relationship by Windpro [5], which is based on comparisons with field measurement data. The black line is based on the model equations (3), (6), and (7). The turbulence intensity as function of (b) the roughness length $z_{0,lo}$, and as function of (c) the boundary layer height for the data shown in panel (a).

and variance

$$\langle\overline{(u'^{+})^2}\rangle = B_1 - A_1 \log(z/\delta), \tag{5}$$

in the boundary layer [28–30].

Equation (4) gives the mean velocity profile in an atmospheric boundary layer, while equation (5) gives the streamwise velocity fluctuations in the boundary layer. Combining both equations gives the turbulence intensity at hubheight as

$$\mathrm{TI}_{\mathrm{hub}} = \frac{[\langle\overline{(u'^{+})^2}\rangle]^{1/2}}{\langle\overline{u}\rangle} = \frac{[B_1 - A_1 \log(z_{\mathrm{h}}/\delta)]^{1/2}}{\kappa^{-1}\ln(z_{\mathrm{h}}/z_{0,\mathrm{lo}})}. \tag{6}$$

The constants A_1 and B_1, are based on those measured in different high Reynolds number turbulent boundary layer experiments, see Marusic *et al.* [28] for an overview. They concluded that $A_1 \approx 1.25$ is an universal constant, while $B_1 \approx 1.5 - 2.1$ depends slightly on the flow geometry. Based on comparisons of our atmospheric boundary layer simulations with experiments we concluded that $B_1 \approx 1.6$ is an appropriate value for this case [30]. According to equation (6) the turbulence intensity at hubheight depends on the roughness length $z_{0,lo}$ and the boundary layer height δ, while equation (3) states that the wake expansion coefficient at hubheight only depends on $z_{0,lo}$.

In addition, we use that the atmospheric boundary layer height is given by [31]

$$\delta = C u_* / f \tag{7}$$

where $f = 2\Omega\sin(\psi)$ with $\Omega = 2\pi/(24 \times 3600s) = 7.27 \times 10^{-5}\ 1/s$, $\psi = 55°$ (the latitude of Horns Rev), and $C = 0.15$, which is typical for neutral atmospheric boundary layers [32–34]. We note that stratification affects the very largest scales the most, i.e. things happening at a height $z = \delta$, but that these effects are much weaker at hubheight, and below (i.e. where $z_{0,lo}$ enters). We verified in the model calculations that small changes in C do not significantly influence the results. Using equations (3), (6), and (7) we obtain for each turbulence intensity the corresponding boundary layer height δ, the roughness height of the ground $z_{0,lo}$, and wake expansion coefficient $k_{w,0}$. Figure 1 shows that the results agree very well with the recommended values by Windpro [5], which are based on comparisons with field measurement data.

2.2. The "top-down" model

In the CWBL model we use the "top-down" approach introduced by Calaf *et al.* [18]. This model is used to obtain the ratio of the mean velocity in the fully develop regime to the reference incoming velocity at hubheight

$$\frac{\langle\overline{u}\rangle(z_\mathrm{h})}{\langle\overline{u_0}\rangle(z_\mathrm{h})} = \frac{\ln\left(\delta_\mathrm{IBL}/z_{0,\mathrm{lo}}\right)}{\ln\left(\delta_\mathrm{IBL}/z_{0,\mathrm{hi}}\right)}\ \ln\left[\left(\frac{z_\mathrm{h}}{z_{0,\mathrm{hi}}}\right)\left(1+\frac{D}{2z_\mathrm{h}}\right)^{\beta}\right]\left[\ln\left(\frac{z_\mathrm{h}}{z_{0,\mathrm{lo}}}\right)\right]^{-1}. \tag{8}$$

Here δ_IBL indicates the height of the internal boundary layer in the fully developed regime of the wind farm, D the turbine diameter, $\beta = \nu_w^*/(1+\nu_w^*)$ and $\nu_w^* \approx 28\sqrt{\pi C_\mathrm{T}/(8 s_\mathrm{x} s_\mathrm{ye})}$, and $z_{0,\mathrm{hi}}$ denotes the roughness length of the wind farm, which is defined as

$$z_{0,\mathrm{hi}} = z_\mathrm{h}\left(1+\frac{D}{2z_\mathrm{h}}\right)^{\beta}\exp\left(-\left[\frac{\pi C_\mathrm{T}}{8 s_\mathrm{x} s_\mathrm{ye}\kappa^2}+\left(\ln\left[\frac{z_\mathrm{h}}{z_{0,\mathrm{lo}}}\left(1-\frac{D}{2z_\mathrm{h}}\right)^{\beta}\right]\right)^{-2}\right]^{-1/2}\right). \tag{9}$$

Here s_ye is the effective spanwise turbine spacing, which is obtained from the two-way coupling with the wake model part of the CWBL model. Due to the two-way coupling between the wake and the "top-down" model s_ye depends on parameters such as the streamwise distance between the turbines s_x, the relative positioning of the turbines, and the wake coefficient in the fully developed regime of the wind farm $k_{\mathrm{w},\infty}$.

The reason for changing the effective spanwise spacing s_ye in the "top-down" model is that this model considers a momentum balance averaged over the entire horizontal plane. In that model the horizontally averaged velocity thus depends on the friction velocity, which depends on the stresses that are imposed by the turbines in the wind farm. However, when the spanwise spacing between the turbines is very large this assumption is not longer valid. This fact can be clearly seen from cases with very small streamwise spacing, s_x, and very large spanwise spacings, s_y, which in the "top-down" model (that only depends on s) will result in limited wake effects. This assumption is obviously unrealistic, as even for a single line of turbines aligned in the wind direction for which $s_\mathrm{y} = \infty$ a significant power reduction is observed for downstream turbines. In the CWBL model we assume that the momentum analysis in the "top-down" part of the model should be performed over the control area that is representative of the region that is directly influenced by the wind turbine wakes. Since the wakes progress very far in the downstream direction, the streamwise spacing, s_x, is unadjusted in the model, while the wake expansion is limited in the spanwise direction. In the CWBL modeling approach the effective spanwise spacing, s_ye, that should be used is obtained from a two-way coupling procedure with a wake model. For further details about this procedure we refer the reader to section IV of Ref. [15].

2.3. Coupling

The wake and "top-down" parts of the CWBL model are coupled by demanding that both models give the same prediction for the turbine velocity in the fully developed regime of the wind farm. An iterative procedure is used to obtain the effective spanwise spacing, s_ye, in equation (9) and the wake expansion rate, $k_{\mathrm{w},\infty}$, in equation (1) in the fully developed regime. The effective spanwise spacing, s_ye, is the spanwise dimension of the control volume size that is used to account for the large scale interactions with the atmosphere as explained above. Because in the wake model the turbine velocity in the fully developed regime depends on $k_{\mathrm{w},\infty}$, while in the "top-down" model this velocity depends on s_ye, these values need to be iterated until convergence is reached and this iteration is accomplished through the two-way coupling in the CWBL model. This procedure is described in detail for aligned and staggered wind farms in Stevens *et al.* [15]. To make sure that the effect of the wind farm geometry is taken into account

this two-way coupling should be enforced for each wind direction separately, which is described in detail in Ref. [22]. Here we in addition, iterate the internal boundary later thickness in the fully developed regime as

$$\delta_{\mathrm{IBL}} = \delta \frac{u_{\mathrm{hi},*}}{u_*}, \tag{10}$$

where

$$\frac{u_{*\mathrm{hi}}}{u_*} = \frac{\ln\left(\delta_{\mathrm{IBL}}/z_{0,\mathrm{lo}}\right)}{\ln\left(\delta_{\mathrm{IBL}}/z_{0,\mathrm{hi}}\right)}. \tag{11}$$

is obtained from the CWBL model. We limit the internal boundary layer thickness to 500 meters when we compare with the LES data (as this was the boundary layer thickness used in the corresponding simulations by Porté-Agel *et al.* [35]) and 1000 meters (height of the thermal inversion) for the comparison with the field measurements.

In order to capture the entrance effects the CWBL model assigns a wake coefficient

$$k_{\mathrm{w,T}} = k_{\mathrm{w},\infty} + (k_{\mathrm{w},0} - k_{\mathrm{w},\infty}) \exp(-\zeta m), \tag{12}$$

to each turbine in the wind farm by interpolating between $k_{\mathrm{w},0}$ (the wake expansion coefficient at the entrance of the wind farm) and $k_{\mathrm{w},\infty}$ (the wake expansion coefficient in the fully developed regime, which is found using the iterative procedure). Here $\zeta = 1$ and m is the number of turbine wakes that interact with the turbine of interest. Thus the wake model part dominates in the entrance region of the wind farm, while the wake development further downstream is determined by the two-way coupling between the wake and "top-down" models that comprise the CWBL model. Therefore the CWBL predictions in the fully developed regime of the wind farm depend much less on the quadratic superposition of the wakes [4] than those of the stand alone wake model.

In this proceeding we assumed that all turbines operate with the same thrust coefficient C_{T}. In the field measurements [25] and the LES results [26] to which we compare the model predictions the wind speeds considered correspond to turbines operating in region II for which this assumption is reasonable. Because the measurement consider a very narrow range of wind speeds we neglected the variation of the power coefficient C_P with wind speed as this effect cancels out when relative powers are considered.

3. Results

Figure 2a shows the layout of the Horns Rev wind farm, which consists of 80 turbines with a hubheight of 70 meters and a turbine diameter of 80 meters, in a rectangular pattern. The streamwise spacing (East-West direction) is 7 turbine diameters and the spanwise spacing (North-South) is 6.95 turbine diameters. Figure 2 shows the power deficits as function of the downstream distance averaged for the wind directions $270^\circ \pm 15^\circ$, $222^\circ \pm 15^\circ$, and $312^\circ \pm 15^\circ$, and a wind speed of 8 ± 0.5 m/s with an average turbulence intensity of 7.0% (6.3% for $222^\circ \pm 15^\circ$) (see figure 4 of Hansen *et al.* [25]). The corresponding model results capture these measurements quite accurately. The figure also shows that the CWBL model agrees well with LES results from Wu and Porté-Agel [26].

The study of Hansen *et al.* [25] also analyzed the effect of turbulence intensity and atmospheric stability on the downstream power development. Hansen *et al.* [25] defined different stability classes ($cL = 3$, $cL = 2$, and $cL \leq 1$) based on the Obukhov length, see table 1 of Ref. [25]. In the remainder of the proceeding we will refer to these different cases using the naming convention introduced by Hansen *et al.* [25], i.e. "very stable" (case label $cL = 3$), "stable" (case label $cL = 2$), and "remaining" (case label $cL \leq 1$). From figure 7 of their paper we obtain that the average turbulence intensity of these three main stability classes they consider are 7.1%, 5.1%, and 3.9%, respectively, when the wind speed is 8 ± 0.5 m/s. We use these reported

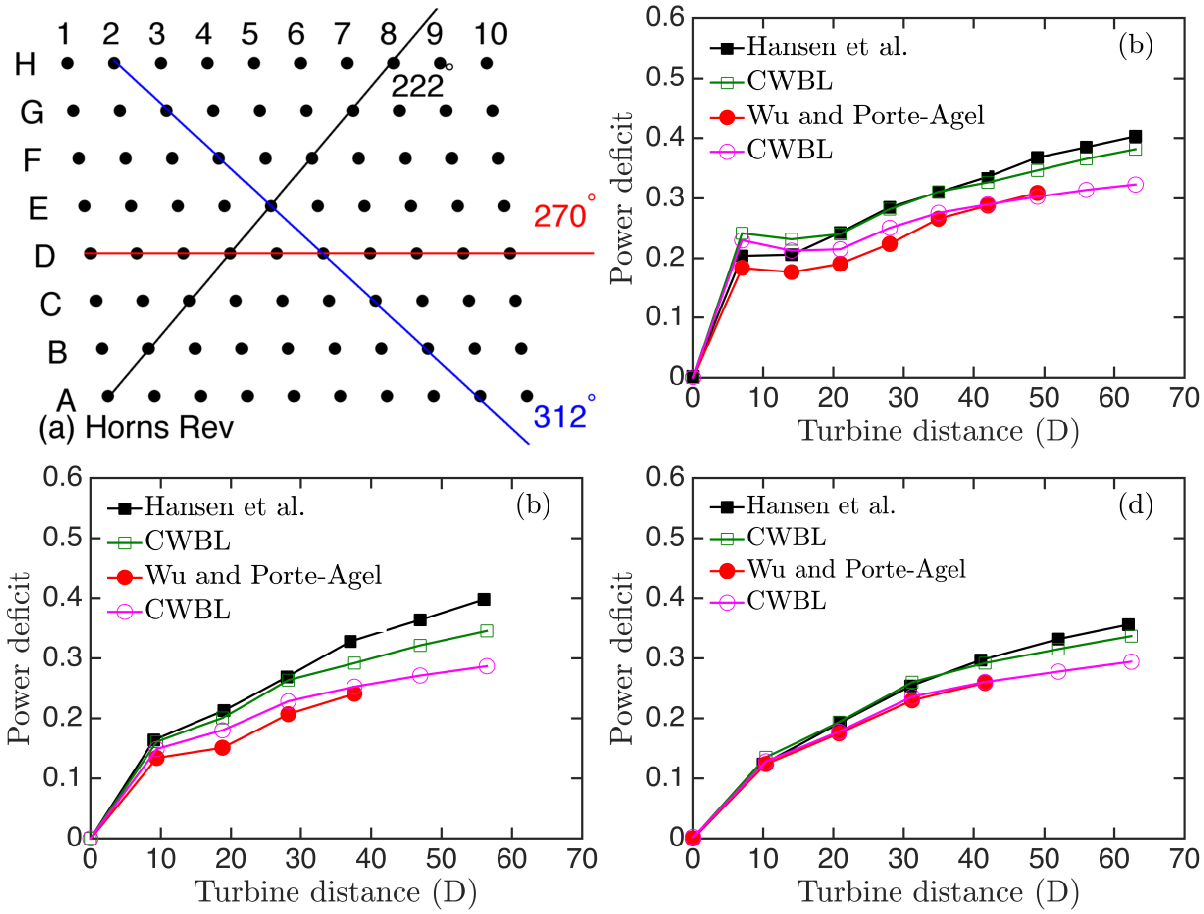

Figure 2. (a) Sketch of the Horns Rev layout indicating the wind directions 270°, 222°, and 312°. (b) The power deficit along the rows of wind turbines for the wind direction sectors $270 \pm 15°$, (c) 222 ± 15, and (d) $312 \pm 15°$. For the Hansen *et al.* [25] data the wind speed range is 8 ± 0.5 m/s with an average turbulence intensity of 7.0% [25] for $270 \pm 15°$ and $312 \pm 15°$, and 6.3% for $222 \pm 15°$. The corresponding CWBL predictions have been computed using a turbine thrust coefficient $C_{\mathrm{T}} = 0.80$. For the LES data of Wu and Porté-Agel [26] the turbulence intensity is 7.7% and we used $C_T = 0.78$ for the corresponding CWBL calculations [22, 26]. The squares provide a comparison between the data from Hansen *et al.* [25] and the CWBL model and the circles between the data from Wu and Porté-Agel [26] and the CWBL model. The data from Hansen *et al.* [25] and Wu and Porté-Agel [26] are digitally extracted from their figures.

turbulence intensities to distinguish the different atmospheric stability classes. We note that the effect of the atmospheric stability is not included in the generalized CWBL model, but that the effect of increasing turbulence intensity is included. Figure 3a shows the measured power deficits for these three stability classes as a function of the downstream direction for the $270 \pm 15°$ direction. Panel (b) of that figure shows the model results for the three corresponding turbulence intensities. The lower panels of figure 3 compare the field experiments and the model results for the three cases separately. In agreement with the experimental observations, the model predicts an increased velocity deficit for decreasing turbulence intensity. The reason is that a higher turbulence intensity results in a wake that better mixes with the surrounding flow. The figure shows that the effect of the turbulence intensity on the wind turbine performance is more pronounced further inside the wind farm.

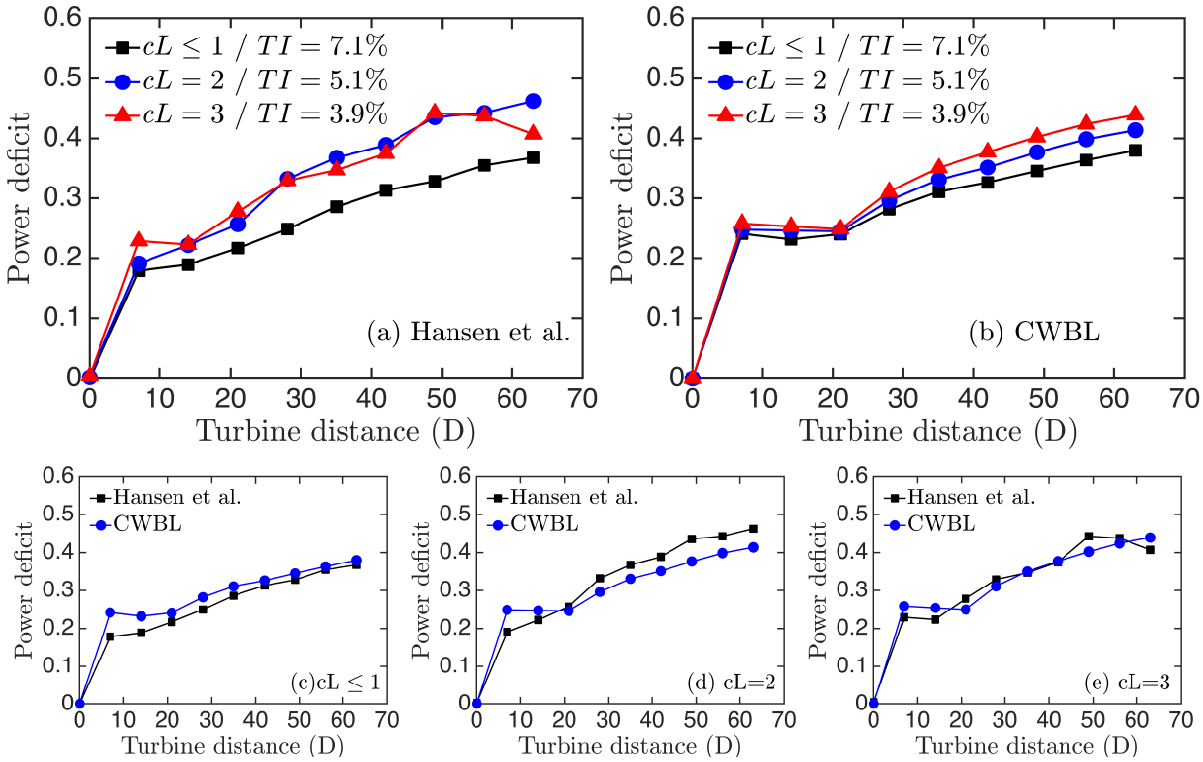

Figure 3. The power deficit along rows of wind turbines with a streamwise spacing of $7D$ averaged for the wind directions $270\pm15°$ and a wind speed of 8 ± 0.5 m/s. The field measurement results are grouped in the very stable ($cL = 3$), stable ($cL = 2$) and remaining ($cL \leq 1$) stability classes. The CWBL predictions have been computed for three different turbulence intensities, i.e. 7.1%, 5.1%, and 3.9%, which correspond to the average turbulence intensity for these three different stability classes. Panels (a) and (b) show a comparison of the three different cases for the field measurements and the CWBL model separately, and panels (c), (d), and (e) compare the field measurements and the corresponding CWBL predictions. The data from Hansen *et al.* [25] are digitally extracted.

Figure 4 shows the same results as in figure 3 for the wind-directions $222\pm15°$ and $312\pm15°$. A comparison with figure 3 reveals that the effect of changes in the turbulence intensity result in similar changes in the wind farm performance for the different wind directions. Considering that the effective streamwise distance is "similar" for these different wind directions (222°, 270°, 312°), i.e. $9.4D$, $7.0D$, and $10.4D$, respectively, and the overall wind turbine density is the same for these cases, this is reasonable. However, the corresponding experimental data seem to indicate a different trend, specifically a bigger influence of the turbulence intensity on the performance for the $222\pm15°$ and $312\pm15°$ cases than for the $270\pm15°$. We do not know the reason for this discrepancy. However, we do note that it is well known in the literature that the comparison with the Horns Rev data to model results tends to be more favorable for some wind-directions than for others [36].

Here we also emphasize that, apart from the turbulence intensity that is included in the model, the effect of the atmospheric stability is not accounted for in the model. So, for example, the effect of the atmospheric thermal stability on the wind shear is not taken into account. Generalizations to this approach can be made by including stability correction functions. Such a direction has been explored in a recent paper dealing with another topic (Sescu & Meneveau

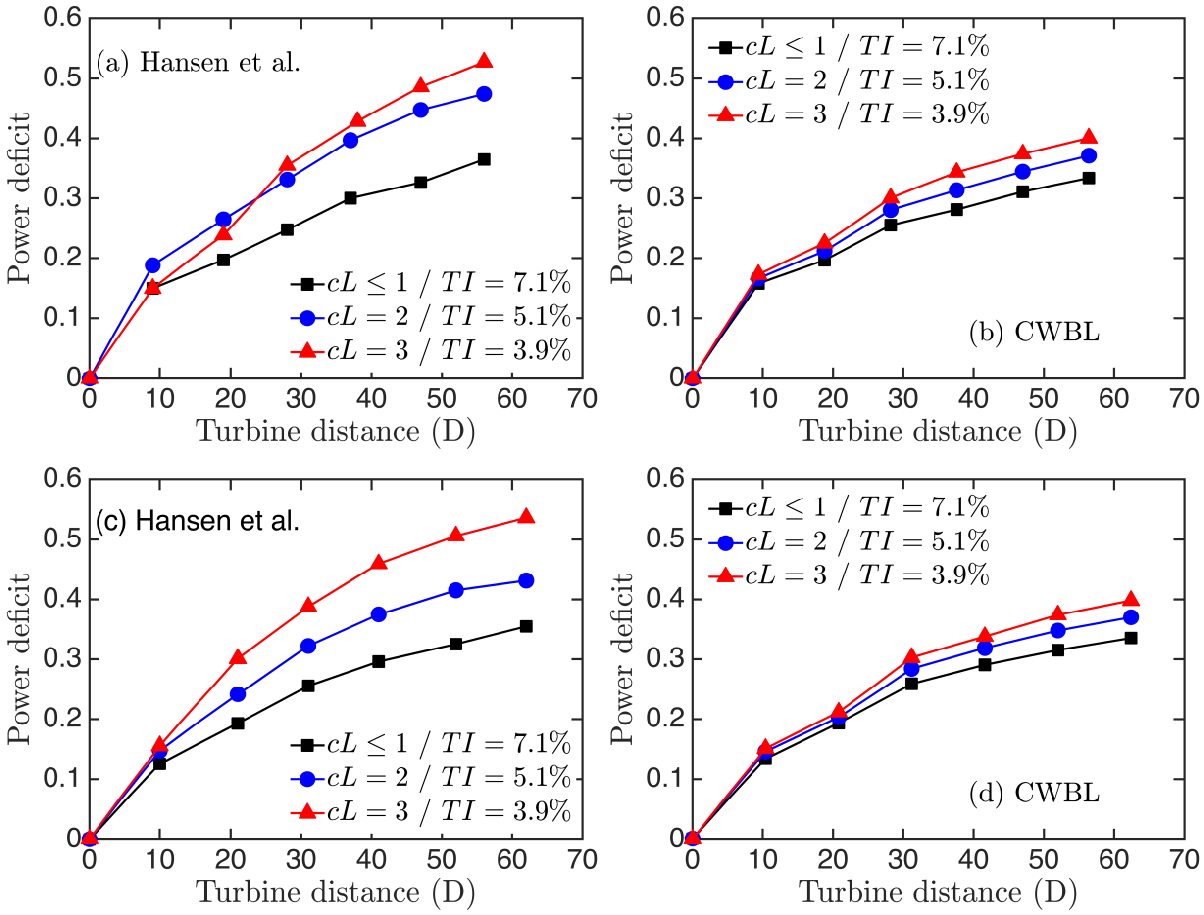

Figure 4. The power deficit for the wind directions $222° \pm 15°$ (top panels) and $312° \pm 15°$ (lower panels) for a wind speed of 8 ± 0.5 m/s. The field measurement results are grouped in the very stable ($cL = 3$), stable ($cL = 2$) and remaining ($cL \leq 1$) stability classes. The CWBL predictions have been computed for three different turbulence intensities, i.e. 7.1%, 5.1%, and 3.9%, which correspond to the average turbulence intensity for these three different stability classes. The left panels indicate the field measurement by Hansen *et al.* [25] and the right panels the CWBL predictions. The data from Hansen *et al.* [25] are digitally extracted.

[37]). Nevertheless the CWBL model is able to predict some of the main trends observed in the field data, which seems to indicates that the change of the turbulence intensity due to the thermal effects is one of the effects that influences the wind farm performance. In the field measurements the effect of the different atmospheric conditions seems stronger for some wind directions.

4. Summary

This paper demonstrates that the predicted performance trends by the coupled wake boundary layer (CWBL) model as a function of the turbulence intensity compare well with trends observed in field measurement data of Horns Rev [25]. The model has been compared with the field experiments using the reported turbulence intensities for the different atmospheric stability classes. We find that the model captures the trend that an increase in the turbulence intensity leads to decreased wake defect velocities due to enhanced mixing. The effect of the turbulence intensity is bigger further downstream. In the model predictions the change in the wind

farm performance due to changes in the turbulence intensity are similar for different wind directions. Considering the similarity between these cases this is reasonable. However, in the field measurements the effect of the different atmospheric conditions seems to be stronger for some wind directions. Further research will be necessary to clarify this behavior. Further research will be necessary to clarify this behavior.

Acknowledgments

RJAMS's work is supported by the program 'Fellowships for Young Energy Scientists' (YES!) of the Foundation for Fundamental Research on Matter (FOM), which is financially supported by the Netherlands Organization for Scientific Research (NWO). Further partial support has been provided by the US National Science Foundation from grant IIA 1243482 (the WINDINSPIRE project).

References

[1] J. F. Herbert-Acero, O. Probst, P.-E. Réthoré, G. C. Larsen, and K. K. Castillo-Villar, *A Review of Methodological Approaches for the Design and Optimization of Wind Farms*, Energies **7**, 6930 (2014).
[2] P. B. S. Lissaman, *Energy Effectiveness of Arbitrary Arrays of Wind Turbines*, J. of Energy **3**, 323 (1979).
[3] N. O. Jensen, *A note on wind generator interaction*, Risø-M-2411, Risø National Laboratory, Roskilde (1983).
[4] I. Katić, J. Højstrup, and N. O. Jensen, *A simple model for cluster efficiency*, European Wind Energy Association Conference and Exhibition, 7-9 October 1986, Rome, Italy 407 (1986).
[5] J. Choi and M. Shan, *Advancement of Jensen (PARK) wake model*, EWEA Conference, Vienna, February 2013 (2013).
[6] A. Peña and O. Rathmann, *Atmospheric stability-dependent infinite wind-farm models and the wake-decay coefficient*, Wind Energy **17**, 1269 (2014).
[7] M. Bastankhah and F. Porté-Agel, *A new analytical model for wind-turbine wakes*, Renewable Energy **70**, 116 (2014).
[8] N. G. Nygaard, *Wakes in very large wind farms and the effect of neighbouring wind farms*, J. Phys. Conf. Ser. **524**, 012162 (2014).
[9] G. Marmidis, S. Lazarou, and E. Pyrgioti, *Optimal placement of wind turbines in a wind park using Monte Carlo simulation*, Renewable Energy **33**, 1455 (2008).
[10] A. Emami and P. Noghreh, *New approach on optimization in placement of wind turbines within wind farm by genetic algorithms*, Renewable Energy **35**, 1559 (2010).
[11] A. Kusiak and Z. Song, *Design of wind farm layout for maximum wind energy capture*, Renewable Energy **35**, 685 (2010).
[12] B. Saavedra-Moreno, S. Salcedo-Sanz, A. Paniagua-Tineo, L. Prieto, and A. Portilla-Figueras, *Seeding evolutionary algorithms with heuristics for optimal wind turbines positioning in wind farms*, Renewable Energy **36**, 2838 (2011).
[13] R. J. Barthelmie, K. Hansen, S. T. Frandsen, O. Rathmann, J. G. Schepers, W. Schlez, J. Phillips, K. Rados, A. Zervos, E. S. Politis, and P. K. Chaviaropoulos, *Modelling and Measuring Flow and Wind Turbine Wakes in Large Wind Farms Offshore*, Wind Energy **12**, 431 (2009).
[14] E. Son, S. Lee, B. Hwang, and S. Lee, *Characteristics of turbine spacing in a wind farm using an optimal design process*, Renewable Energy **65**, 245 (2014).
[15] R. J. A. M. Stevens, D. F. Gayme, and C. Meneveau, *Coupled wake boundary layer model of wind-farms*, J. Renewable and Sustainable Energy **7**, 023115 (2015).
[16] S. Frandsen, *On the wind speed reduction in the center of large clusters of wind turbines*, J. Wind Eng. and Ind. Aerodyn. **39**, 251 (1992).
[17] S. Frandsen, R. Barthelmie, S. Pryor, O. Rathmann, S. Larsen, J. Højstrup, and M. Thøgersen, *Analytical modelling of wind speed deficit in large offshore wind farms*, Wind Energy **9**, 39 (2006).
[18] M. Calaf, C. Meneveau, and J. Meyers, *Large eddy simulations of fully developed wind-turbine array boundary layers*, Phys. Fluids **22**, 015110 (2010).
[19] J. Meyers and C. Meneveau, *Optimal turbine spacing in fully developed wind farm boundary layers*, Wind Energy **15**, 305 (2012).
[20] R. J. A. M. Stevens, *Dependence of optimal wind-turbine spacing on wind-farm length*, Wind Energy DOI: 10.1002/we.1857 (2015).
[21] R. J. A. M. Stevens, D. F. Gayme, and C. Meneveau, *Effects of turbine spacing on the power output of extended wind-farms*, Wind Energy DOI: 10.1002/we.1835 (2015).

[22] R. J. A. M. Stevens, D. F. Gayme, and C. Meneveau, *Generalized coupled wake boundary layer model: applications and comparisons with field and LES data for two real wind farms*, Submitted to Wind Energy (2015).
[23] X. Yang and F. Sotiropoulos, *Analytical model for predicting the performance of arbitrary size and layout wind-farms*, preprint (2014).
[24] C. Meneveau, *The top-down model of wind farm boundary layers and its applications*, J. of Turbulence **13**, 1 (2012).
[25] K. S. Hansen, R. J. Barthelmie, L. E. Jensen, and A. Sommer, *The impact of turbulence intensity and atmospheric stability on power deficits due to wind turbine wakes at Horns Rev wind farm*, Wind Energy **15**, 183 (2012).
[26] Y.-T. Wu and F. Porté-Agel, *Modeling turbine wakes and power losses within a wind farm using LES: An application to the Horns Rev offshore wind farm*, Renewable Energy **75**, 945 (2015).
[27] X. Yang, S. Kang, and F. Sotiropoulos, *Computational study and modeling of turbine spacing effects in infinite aligned wind farms*, Phys. Fluids **24**, 115107 (2012).
[28] I. Marusic, J. Monty, M. Hultmark, and A. Smits, *On the logarithmic region in wall turbulence*, J. Fluid Mech. **716**, R3 (2013).
[29] C. Meneveau and I. Marusic, *Generalized logarithmic law for high-order moments in turbulent boundary layers*, J. Fluid Mech. **719**, R1 (2013).
[30] R. J. A. M. Stevens, M. Wilczek, and C. Meneveau, *Large eddy simulation study of the logarithmic law for high-order moments in turbulent boundary layers*, J. Fluid Mech. **757**, 888 (2014).
[31] C. Rossby and R. Montgomery, *The layers of frictional influence in wind and ocean currents*, Pap. Phys. Oceanogr. Meteor. **3**, 1 (1935).
[32] P. Seibert, F. Beyrich, S.-E. Gryning, S. Joffre, A. Rasmussen, and P. Tercier, *Mixing height determination for dispersion modelling*, Cost Action 710: Preprocessing of Meteorological data for dispersion modeling. Report of Working Group 2 (1997).
[33] A. Peña, S.-E. Gryning, and C. Hasager, *Measurements and Modelling of the Wind Speed Profile in the Marine Atmospheric Boundary Layer*, Boundary-Layer Meteorol **129**, 479 (2008).
[34] A. Peña, S.-E. Gryning, and C. Hasager, *Comparing mixing-length models of the diabatic wind profile over homogeneous terrain*, Theor Appl Climatol **100**, 325 (2010).
[35] F. Porté-Agel, Y.-T. Wu, and C.-H. Chen, *A Numerical Study of the Effects of Wind Direction on Turbine Wakes and Power Losses in a Large Wind Farm*, Energies **6**, 5297 (2013).
[36] R. J. Barthelmie, S. T. Frandsen, O. Rathmann, K. Hansen, E. Politis, J. Prospathopoulos, J. G. Schepers, K. Rados, D. Cabezón, W. Schlez, A. Neubert, and M. Heath, *Flow and wakes in large wind farms: Final report for UpWind WP8*, Report number Risø-R-1765(EN) (2011).
[37] A. Sescu and C. Meneveau, *Large Eddy Simulation and single column modeling of thermally stratified wind-turbine arrays for fully developed, stationary atmospheric conditions*, J. Atmospheric and Oceanic Technology, http://dx.doi.org/10.1175/JTECH-D-14-00068.1 (2015).